

REPORT DOCUMENTATION PAGE			Form Approved OMB No. 0704-0188		
<p>Public reporting burden for this collection of information is estimated to average 1 hour per response, including the time for reviewing instructions, searching existing data sources, gathering and maintaining the data needed, and completing and reviewing this collection of information. Send comments regarding this burden estimate or any other aspect of this collection of information, including suggestions for reducing this burden to Department of Defense, Washington Headquarters Services, Directorate for Information Operations and Reports (0704-0188), 1215 Jefferson Davis Highway, Suite 1204, Arlington, VA 22202-4302. Respondents should be aware that notwithstanding any other provision of law, no person shall be subject to any penalty for failing to comply with a collection of information if it does not display a currently valid OMB control number. <b>PLEASE DO NOT RETURN YOUR FORM TO THE ABOVE ADDRESS.</b></p>					
1. REPORT DATE (DD-MM-YYYY) March 2013		2. REPORT TYPE Technical Paper		3. DATES COVERED (From - To) March 2013-May 2013	
4. TITLE AND SUBTITLE Post-Vitrification Cure Kinetics of High Temperature Composite Resins: Implications for Characterization and Performance			5a. CONTRACT NUMBER In-House		
			5b. GRANT NUMBER		
			5c. PROGRAM ELEMENT NUMBER		
6. AUTHOR(S) Andrew Guenther, Josiah Reams, Christopher Sahagun, Matthew Davis, Joseph Mabry			5d. PROJECT NUMBER		
			5e. TASK NUMBER		
			5f. WORK UNIT NUMBER Q0BG		
7. PERFORMING ORGANIZATION NAME(S) AND ADDRESS(ES)  Air Force Research Laboratory (AFMC) AFRL/RQRP 10 E. Saturn Blvd. Edwards AFB CA 93524-7680			8. PERFORMING ORGANIZATION REPORT NO.		
9. SPONSORING / MONITORING AGENCY NAME(S) AND ADDRESS(ES) Air Force Research Laboratory (AFMC) AFRL/RQR 5 Pollux Drive Edwards AFB CA 93524-7048			10. SPONSOR/MONITOR'S ACRONYM(S)		
			11. SPONSOR/MONITOR'S REPORT NUMBER(S) AFRL-RQ-ED-TP-2013-008		
12. DISTRIBUTION / AVAILABILITY STATEMENT Distribution A: Approved for Public Release; Distribution Unlimited. PA#13090					
13. SUPPLEMENTARY NOTES Conference paper for the 2013 International SAMPE Meeting, Long Beach, CA, 6-9 May 2013.					
14. ABSTRACT Many high-temperature composite resins, such as cyanate esters, require high temperatures in order to achieve complete cure. In such situations, incomplete conversion often persists in completely solidified "cured" samples, leading to potentially significant degradation in performance. Moreover, the very steep dependence of the glass transition temperature of the composite resin on the extent of cure leads to unusual cure effects such as 1) significant cure below the glass transition temperature 2) cure kinetics that involve extremely strong temperature dependence coupled with very weak dependence on cure time, and 3) unexpected conversion-property relationships (e.g. a decrease in elastic modulus with increasing extent of cure). These effects not only complicate the prediction of composite performance, they also make the determination of even simple properties such as the extent of conversion or glass transition temperature prone to large, difficult-to-detect errors. This paper describes and demonstrates newly developed characterization methods that combine multiple techniques to overcome these difficulties, and allow for a more complete description of the evolving glass transition temperature of composite resins during part fabrication, testing, and performance. In addition, the paper describes how insights into the unusual phenomena associated with resins that cure at high temperature can lead to design strategies for high-temperature composite resins that provide optimal performance.					
15. SUBJECT TERMS					
16. SECURITY CLASSIFICATION OF:			17. LIMITATION OF ABSTRACT	18. NUMBER OF PAGES	19a. NAME OF RESPONSIBLE PERSON Joseph Mabry
a. REPORT Unclassified	b. ABSTRACT Unclassified	c. THIS PAGE Unclassified			19b. TELEPHONE NO (include area code) 661-525-5857

# POST-VITRIFICATION CURE KINETICS OF HIGH TEMPERATURE COMPOSITE RESINS: IMPLICATIONS FOR CHARACTERIZATION AND PERFORMANCE

Andrew J. Guenther,<sup>1</sup> Josiah T. Reams,<sup>2</sup> Christopher M. Sahagun,<sup>3</sup> Matthew C. Davis,<sup>4</sup>  
and Joseph M. Mabry<sup>1</sup>

<sup>1</sup>Aerospace Systems Directorate, Air Force Research Laboratory, Edwards AFB, CA 93524

<sup>2</sup>ERC Incorporated, Edwards AFB, CA 93524

<sup>3</sup>National Research Council / Air Force Research Laboratory, Edwards AFB, CA 93524

<sup>4</sup>Naval Air Warfare Center, Weapons Division, China Lake, CA 93555

## ABSTRACT

Many high-temperature composite resins, such as cyanate esters, require high temperatures in order to achieve complete cure. In such situations, incomplete conversion often persists in completely solidified “cured” samples, leading to potentially significant degradation in performance. Moreover, the very steep dependence of the glass transition temperature of the composite resin on the extent of cure leads to unusual cure effects such as 1) significant cure below the glass transition temperature 2) cure kinetics that involve extremely strong temperature dependence coupled with very weak dependence on cure time, and 3) unexpected conversion-property relationships (e.g. a decrease in elastic modulus with increasing extent of cure). These effects not only complicate the prediction of composite performance, they also make the determination of even simple properties such as the extent of conversion or glass transition temperature prone to large, difficult-to-detect errors. This paper describes and demonstrates newly developed characterization methods that combine multiple techniques to overcome these difficulties, and allow for a more complete description of the evolving glass transition temperature of composite resins during part fabrication, testing, and performance. In addition, the paper describes how insights into the unusual phenomena associated with resins that cure at high temperature can lead to design strategies for high-temperature composite resins that provide optimal performance.

## 1. INTRODUCTION

The need to produce affordable high-performance composite structures for microelectronics, aerospace, and energy applications has led to the continuing development of polymer composite resins that combine a high maximum use temperature with simple processing methods. In terms of glass transition temperature ( $T_G$ ), these two competing demands are contradictory. On one hand, because mechanical stability is required in service, a high maximum use temperature requires that the glass transition temperature of the resin exceed the maximum use temperature, therefore resins with a high  $T_G$  are needed. On the other hand, low viscosity liquids are the easiest materials to process, and a lower viscosity is most readily achieved in the liquid state by lowering either the melting or vitrification temperature (another name for  $T_G$ ) as much as possible.

Fortunately, these competing demands can be satisfied simply by developing resin systems in which monomers having a  $T_G$  well below room temperature are converted to macromolecular

Distribution A: Approved for public release; distribution unlimited. This paper is declared a work of the U. S. Government and is not subject to copyright protection in the United States.

networks having a very high  $T_G$ . Such behavior is a key characteristic of many high-temperature composite resins including cyanate esters, benzoxazines, and even high-temperature epoxy resins. Among these, cyanate ester resins [1-3] are among the most convenient for study, because of the simplicity of the cure reaction that involves formation of a single product [4] that is readily identified and distinguished from side products [5] even in the vitrified, insoluble form, and which does not require consideration of stoichiometric effects.

The transition from low to high  $T_G$  in thermosetting resins such as cyanate esters is described by the diBenedetto equation [6,7]. This simple equation is quite powerful in that it provides for a direct, one-to-one, quantitative relationship between conversion and glass transition temperature. Such a relationship is only valid for systems such as cyanate esters in which reaction intermediates are present only at low levels and which form a single, well-defined type of cross-link in the cured macromolecular network. The form of the diBenedetto equation is:

$$\frac{T_G - T_{G0}}{T_{G\infty} - T_{G0}} = \frac{\lambda\alpha}{1 - (1 - \lambda)\alpha} \quad (1)$$

In which  $T_G$ ,  $T_{G0}$  and  $T_{G\infty}$  represent the glass transition temperatures of the partially cured polymer, monomer, and fully cured network respectively, while the conversion  $\alpha$  represents the fraction of monomer groups that have reacted, and  $\lambda$  is an adjustable parameter that typically takes on values of 0.25 – 0.45 for cyanate esters[5,8].

The left hand side of Eq. (1) represents a dimensionless temperature (herein denoted  $\theta$ ), with a characteristic temperature range ( $T_{G\infty} - T_{G0}$ ) herein denoted as  $T^*$ . The quantity  $T^*/\lambda$  (herein denoted  $S^*$ ) represents the characteristic sensitivity of the glass transition temperature to conversion. As  $\alpha \rightarrow 1$ ,  $dT_G/d\alpha \rightarrow S^*$ ; moreover, a plot of  $1/(T_G - T_{G0})$  vs.  $1/\alpha$  is expected to feature a slope of  $S^*/T^{*2}$  and an intercept of  $(S^* - T^*)/T^{*2}$ . Note that  $S^*$  and  $T^*$  both have units of temperature.

The development of high-temperature thermosetting resins that retain favorable processing characteristics may thus be described as maximization of  $T^*$ . Since  $\lambda$  is an empirical parameter that does not vary over a wide range, in general, efforts to maximize  $T^*$  have also resulted in much larger values of  $S^*$ . In this paper, the consequences of large values for  $S^*$  for the determination of the properties of thermosetting resins are explored. Large values of  $S^*$  magnify the importance of phenomena such as vitreous cure and *in-situ* cure during measurement, which are often ignored on the grounds that they are insignificant. Using high-temperature cyanate esters, which have some of the largest known  $T^*$  and  $S^*$  values of any thermosetting resin, we illustrate how significant the effects of *in-situ* and vitreous cure can be, and discuss methods that take into account these effects when determining or utilizing physical property data.

## 2. EXPERIMENTATION

### 2.1 Materials

The dicyanate ester of Bisphenol A (Primaset® BADCy) was purchased from Lonza and used as received. ESR-255, an experimental cyanate ester first reported by Shimp [9] and more recently synthesized at NAWCWD and sent to AFRL for comparative studies [10], was also utilized extensively due to its very high  $T^*$  and  $S^*$  values. Nonylphenol (technical grade) was purchased from Aldrich, and Copper (II) acetylacetonate was purchased from ROC/RIC; both were used as received. Chemical structures are provided in Figure 1. All BADCy samples utilized in this study were catalyzed, while all ESR-255 samples were uncatalyzed.

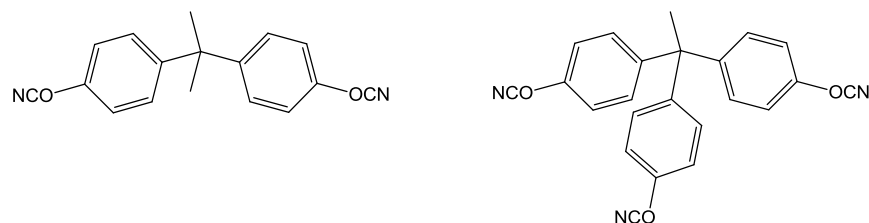


Figure 1. Chemical structures of the cyanate ester monomers studied: (left) BADCy, and (right) ESR-255

## 2.2 Sample Preparation

For catalyzed samples, batches of catalyst comprised of 30 parts by weight nonylphenol to one part by weight of copper (II) acetylacetonate were prepared by mixing the ingredients in a vial and heating to 60°C while stirring vigorously until complete dissolution took place (typically one to two hours). These batches were retained for up to 30 days.

For BADCy, uncured samples for differential scanning calorimetry (DSC) analysis were prepared by melting and mixing the monomer with 2 parts per hundred by weight of catalyst at 95°C. For ESR-255 samples, the monomer was melted at a temperature of 120-130 °C with no added catalyst. 3-5 mgs of the molten samples were then sealed in non-hermetic DSC pans for analysis.

## 2.3 Characterization Techniques

DSC was performed on a TA Instruments Q2000 calorimeter under 50 mL/min. of flowing nitrogen. For catalyzed BADCy samples, two sets of protocols were used. In the first set, samples were heated at 5 °C / min. to 150 °C then held at 150 °C for 60, 120, or 720 min. to accomplish partial cure. The samples were then quenched by cooling at 20 °C / min. to 0 °C, heated at 10 °C / min. to 350 °C to complete residual cure, then cooled at 20 °C / min. to 25 °C and heated once again at 10 °C / min. to 350 °C in order to provide a re-scanned baseline for the residual cure. For the isothermal cure segments as well as the heating segments prior to isothermal cure, the baseline was chosen manually at a constant value consistent with the signal below the melting transition (for the heating segments) or at the longest available times (for isothermal segments), both of which reflect the samples at their most inactive states where the rate of cure should be near zero. Data for the samples cured for 720 minutes has been published elsewhere [5].

For the ESR-255 sample, a more sophisticated technique was utilized since the sample was part of a previously reported study [10] on cure kinetics and physical properties. In this method, the sample was heated to 120 °C at 5 °C / min. and allowed to equilibrate for 5 min. Following this, the sample was heated as rapidly as possible (about 100 °C / min.) to 250 °C, then held at 250 °C for 240 min. Next, the sample was quenched by cooling as rapidly as possible (50 – 100 °C / min.) to 125 °C. After quenching, residual cure was completed by heating the sample at 10 °C / min. to 350 °C. Following this, the sample was cooled at 10 °C / min. to 120 °C and equilibrated for 5 min. The isothermal (with rapid temperature jump), quenching, and re-heating steps were then repeated just as before to generate a re-scanned baseline for the entire run. Additional data for this sample have been published previously [10].

In accordance with the study of baseline techniques described in Supporting Information, Section S6.3.1, of Reference 10, an offset, equal to the minimum observed raw value of the re-scanned minus original heat flow values, was added to the re-scanned baseline in all non-isothermal segments. In the case of BADCy cured at 200 °C, an unusual transient in the DSC signal

required the use of an estimated offset based on the step size of the  $T_G$  signal in the fully-cured sample.

For each DSC scan, the sample conversion at every point during the scan was calculated as follows. First, it was assumed that no cure occurred prior to or during sample melting for catalyzed BADCy, and no cure occurred prior to the temperature jump for the uncatalyzed ESR-255 sample. It was further assumed that no cure took place during quenching, or below the clearly visible glass transition temperature during the residual scan of the catalyzed BADCy samples. Because the re-scan was used to compute the baseline, it was also automatically assumed (as a consequence of the method) that no cure took place during the re-scan. At every point during the scan for which it was assumed that cure was possible, the measured heat flow was subtracted from the appropriate baseline value and divided by sample mass.

The heat flow per unit mass values were then integrated using a simple rectangular rule with typical time steps being 3-15 seconds in length (and forward time steps, that is, the time difference between points “i” and “i+1” was paired with the value at point “i”) in order to generate a running total of the evolved heat of reaction. For BADCy samples, the total heat of reaction was simply taken to be the value of the running total at the end of the residual heating step, since combined DSC / IR studies (see Section 3 of Supporting Information in Reference 10) indicate that no significant uncured material remains after heating to 350 °C. For ESR-255, similar DSC / IR studies (also reported in Section 3 of Supporting Information in Reference 10) establish that heating to 350 °C does not provide complete cure, and that a more appropriate measure of the total heat of reaction is simply to use the fixed value of 110 kJ/eq. (or 866 J/g), and to utilize the integrated heat of melting for the sample to provide an accurate measurement of the sample mass. These steps were followed with the ESR-255 sample described herein.

Once the total heat of reaction ( $\Delta H_{total}$ ) was measured, the conversion ( $\alpha$ ) was obtained at every point using the formula

$$\alpha = \frac{\Delta H_{total} - \Delta H_{0-i}}{\Delta H_{total}} \quad (2)$$

in which  $\Delta H_{0-i}$  represents the running total of all the heat flow per unit mass values up to point “i”. Once computed, the estimated value of  $T_G$  at every point was computed simply by applying the diBenedetto formula (Eq. 1) to the conversions at every point. The estimated conversion rates and estimates of  $dT_G/dt$  were computed using a simple linear difference formula over a window of five points centered at point “i”

### 3. RESULTS

Table 1 lists the estimated diBenedetto equation parameters and consequent  $T^*$  and  $S^*$  values for BADCy and ESR-255, together with their uncertainties. Note that the uncertainty estimate for the parameter  $\lambda$  for ESR-255 was obtained by a brief re-examination of the data in Section S4.3.3 of Reference 10. Changes of 0.02 in the value of  $\lambda$  led to a fit that appeared little different from the one presented, while changes of 0.04 led to a marginal fit and changes of 0.08 led to a clearly poor fit, thus 0.04 was selected as the characteristic uncertainty. A similar approach led to the error estimates for the other parameters. Error estimates for  $T^*$  and  $S^*$  were determined by simple propagation of error, assuming no correlation between the factors. The uncertainty in  $\lambda$  alone differs from the total uncertainty in  $S^*$  by less than 1% for BADCy and 13% for ESR-255, thus error estimates can be greatly simplified by substituting uncertainty in  $\lambda$  for uncertainty in all three diBenedetto equation parameters when computing the uncertainty in quantities that depend on all three diBenedetto equation parameters.

Table 1. Key diBenedetto equation parameters for BADCy and ESR-255.

Parameter	BADCy Value	ESR-255 Value
$T_{G0}$	$-38 \pm 1$ °C	$-9 \pm 10$ °C
$T_{G\infty}$	$300 \pm 3$ °C	$558 \pm 40$ °C
$\lambda$	$0.38 \pm 0.04$	$0.32 \pm 0.04$
$T^*$	$338 \pm 3$ °C	$570 \pm 40$ °C
$S^*$	$890 \pm 90$ °C	$1800 \pm 300$ °C

The sensitivity parameters ( $S^*$ ) in Table 1 can be interpreted as follows. The  $T_G$  of BADCy near full cure increases by about 9 °C for every 1% increase in conversion, while that of ESR-255 increases by roughly twice as much, or roughly 18 °C for every 1% increase in conversion. Note, however, that because  $T_{G\infty}$  for ESR-255 at full cure is above the short-term decomposition temperature, in essence, full conversion is not physically realizable since it would require deforming the chemical bonds in the network beyond their breaking point. The inability to achieve full conversion also is what leads to the much higher uncertainties in individual diBenedetto equation parameters for ESR-255.

### 3.1 Isothermal Cure Experiments

As mentioned in Section 2.3, through the diBenedetto equation it is possible to track the  $T_G$  of cyanate esters during DSC experiments. One of the simplest ways to explore the relationships between cure temperature and  $T_G$  in cyanate ester resins is therefore through isothermal cure DSC experiments. However, a key question that must be answered is whether the uncertainty in the estimate of  $T_G$  is small enough to allow for meaningful interpretation of the data.

Figure 2 shows the sample temperature, measured raw heat flow, and estimated  $T_G$  in a typical isothermal DSC experiment. The material used in this case is catalyzed BADCy with an isothermal cure temperature of 150 °C and a dwell time of 12 hours.

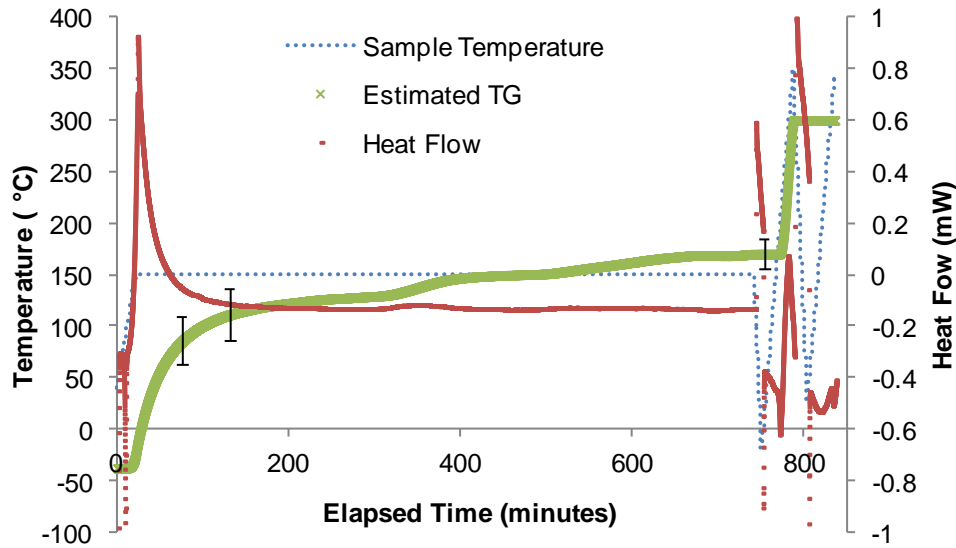


Figure 2. Overview of isothermal cure DSC experiment for catalyzed BADCy held at 150 °C for 12 hours.

After the isothermal cure, the sample is quenched, then re-heated to 350 °C to achieve full cure, at which point  $T_G = T_{G\infty}$  by definition. After quenching again, the heating cycle is repeated in order to generate a “re-scanned baseline”, an approach successfully used by Kessler [8] and shown to produce high-precision heat flow measurements in recent work by us [10]. For the

preceding portions of the experiment, the baseline must be drawn manually. For the long isothermal period, an examination of the signal near the end of the isothermal portion enables the baseline to be estimated with an error of no more than 0.005 mW. For the earlier, initial heating portions, the baseline can be estimated from the low-temperature portion of the curve prior to the initiation of cure, with an error also of about 0.005 mW. The re-scanned baseline has a somewhat larger error, near 0.02 mW, due to the alteration of the location of the step associated with the  $T_G$  of the sample as well as small changes in sample heat capacity during residual cure. Although in principle these effects can be accounted for, to do so for the purpose of tracking  $T_G$  would make data analysis unnecessarily cumbersome given the magnitude of other factors contributing to the uncertainty in the  $T_G$  estimate.

In Table 2, the effects of the uncertainties discussed above on the estimated conversion and  $T_G$  of the BADCy sample at three points (60, 120, and 720 minutes) during the 720-minute isothermal cure depicted in Figure 2 are listed, based on a sensitivity analysis done with the baselines and diBenedetto parameter  $\lambda$  used in estimating heat flows and  $T_G$  values. Note that the actual (not estimated)  $T_G$  at  $168 \pm 1$  °C (published previously [5]) at the end of the isothermal cure can be seen in the DSC signal during the post-cure heating segment. To determine the actual  $T_G$  after 60 and 120 minutes, experiments like the one depicted in Figure 2 were undertaken with total cure times of 60 and 120, rather than 720, minutes, and the actual  $T_G$  during the post-cure heating segment was recorded.

Table 2. Sensitivity analysis for DSC experiment depicted in Figure 2.

Variation	60 min.		120 min.		720 min.	
	$\alpha$	$T_G$ (°C)	$\alpha$	$T_G$ (°C)	$\alpha$	$T_G$ (°C)
None (as modeled)	0.616	90	0.682	114	0.808	170
Initial non-iso manual baseline +0.005 mW	0.615	90	0.681	113	0.808	170
Initial non-iso manual baseline -0.005 mW	0.617	90	0.682	114	0.809	170
Iso. manual baseline +0.005 mW	0.681	113	0.745	140	0.785	158
Iso. manual baseline -0.005 mW	0.564	73	0.631	95	0.827	180
Re-scanned baseline +0.02 mW	0.622	92	0.689	116	0.817	175
Re-scanned baseline -0.02 mW	0.610	88	0.675	111	0.800	166
$\lambda +0.04$	0.616	98	0.682	122	0.808	178
$\lambda -0.04$	0.616	81	0.682	105	0.808	161
Observed $T_G$	--	110	--	144	--	168

Based on the data in Table 2, the major sources of uncertainty in the estimated  $T_G$  are the uncertainty in the baseline value for the isothermal segment and the uncertainty in diBenedetto equation parameters (represented, as explained earlier, by variation in  $\lambda$ ). The former affects both conversion and  $T_G$  values, whereas the latter affects only  $T_G$  values. Because conversion estimates are based on cumulative heat flow measurements, the sensitivity to the baseline value is directly proportional to the length of time covered by the baseline. Thus, for 720-minute isothermal cure experiments, it is expected that the results will be highly sensitive to the isothermal baseline value. Interestingly, though, the resultant uncertainty diminishes markedly as the cure time progresses. This is because the measured conversion represents a fraction in which the area under the heat flow curve for all elapsed segments is divided by under the area of the curve for all segments. Late in the isothermal cure period, the cumulative effect of baseline variations is large in both the numerator (elapsed segments) and denominator (all segments), and the effects, provided they are reasonably small, cancel to a significant extent. Early in the isothermal segment, the elapsed time is small, so the effect of baseline variation is small in the numerator but large in the denominator, making for a significant change in the fractional value

(that is, the conversion). The end result is that, for long isothermal segments, baseline variations affect the modeled  $T_G$  value near the end of the segment about as much as do diBenedetto equation parameter uncertainties, however, the shape of the estimated  $T_G$  curve during the early part of the segment is highly sensitive to the choice of baseline.

A careful examination of Figure 2 reveals these effects. At about 350 minutes, there is a small fluctuation in the baseline, which causes a marked change in the estimated  $T_G$  value. Even though the  $T_G$  value at the end of the segment is quite close to the experimentally observed one, the shape of the curve at early times is less certain. The error bars in Figure 2 are produced by taking into account the two largest sources of error identified in the sensitivity analysis (in this case, the isothermal baseline and the diBenedetto equation parameters) and treating them as independent sources of error. The resultant error bars are large at early times and shrink at later times, due to the fractional measurement effects described earlier. The error bars clearly show that the shape of the curve (which would determine isothermal kinetic exponents) would be highly sensitive to the baseline choice, a fact that has previously been noted by Hamerton [11]. Note also that the errors being discussed are systematic, rather than random, errors. Hence, for derived parameters, such as conversion rates, a sensitivity analysis rather than propagation of error calculations were used to determine the error bars shown in subsequent figures for derived parameters such as the rate of  $T_G$  increase. These sensitivity analyses utilized the two largest sources of error, one of which was always the diBenedetto equation parameters (represented by variation in  $\lambda$ ) and the other, assumed independent, was either the isothermal (for long isothermal scans) or re-scanned (for shorter isothermal scans) baseline variation.

While the preceding analysis provides insights into the precision of the  $T_G$  estimates, because many of the errors are systematic, it is important to consider accuracy as well. To do this, five different isothermal DSC experiments were performed involving cure times of 60, 120, and 720 minutes at 150 °C, or 60 minutes at 150 °C followed by either 30 or 720 minutes at 200 °C. An actual  $T_G$  value was observed at the end of these experiments and compared to the estimated value for the corresponding cure condition. For all these experiments, catalyzed BADCy was used. As an example, consider the 720-minute cure at 200 °C, illustrated in Figure 3. Since this sample was also cured for 60 minutes at 150 °C, the  $T_G$  after 60 minutes at 150 °C can be estimated and compared to the observed value (from the DSC experiment in which only this cure step was performed). In the same way, the  $T_G$  after 30 minutes at 200 °C (including the preceding 60 minutes at 150 °C) may also be estimated and compared to the observed value from the appropriate DSC run. Lastly, the estimated  $T_G$  after 720 minutes at 200 °C can be compared to the observed value (in this case from the same DSC run). Using these five experiments, a total of 11 comparisons of predicted and experimental  $T_G$  values were made. These are displayed in Table 3, including the uncertainty estimates for predicted  $T_G$  values generating using the methods described earlier.

Table 3. Comparison of estimated and observed  $T_G$  values for catalyzed BADCy

Source (Pred. from iso. DSC run, or “observed”)	$T_G$ after curing for temp. (°C) / time (min.)				
	150/60	150/120	150/720	200/30*	200/720*
Pred. 150 °C / 60 min.	107 ± 9	--	--	--	--
Pred. 150 °C / 1200 min.	114 ± 9	143 ± 9	--	--	--
Pred. 150 °C / 720 min.	90 ± 22	114 ± 24	170 ± 14	--	--
Pred. 200°C / 30 min.*	113 ± 9	--	--	174 ± 9	--
Pred. 200°C / 720 min.*	120 ± 22	--	--	192 ± 36	229 ± 8
Observed $T_G$	110	144	168	206	246

\* Note that all cures at 200 °C include a previous cure step at 150 °C for 60 minutes



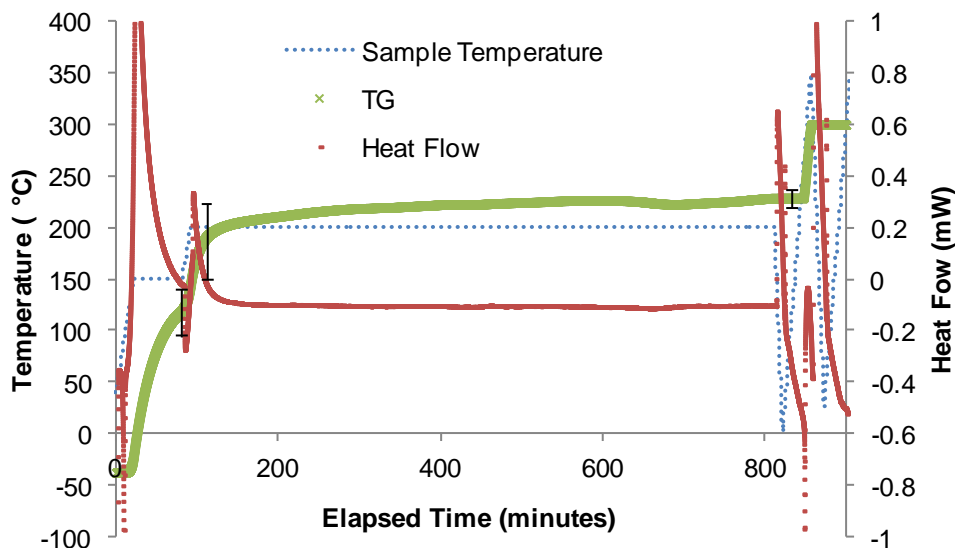


Figure 3. Overview of isothermal cure DSC experiment for catalyzed BADCy held at 150 °C for 1 hour, followed by holding at 200 °C for 12 hours.

A few tentative conclusions may be drawn from Table 3. First, for relatively short isothermal segments with a single cure temperature, the predictions are quite good. As expected, the effect of baseline error results in lower quality predictions, and correspondingly poorer agreement with experiment for the long cure steps. Interestingly, though, the long cure runs are needed to establish the true baseline values, since during the shorter steps, cure is on-going throughout the segment, and a careful examination shows that no true baseline is apparent (one might easily estimate the baseline incorrectly in these situations, assuming that cure stops completely simply because it slows down greatly). The predictions at 200 °C also appear considerably less accurate and systematically low. One likely reason is that it is not possible to manually determine true baselines for the intermediate steps (in these cases, the other manual baselines for non-isothermal and isothermal segments, respectively, were assumed to apply to the corresponding non-isothermal and isothermal intermediate steps). Thus, the use of less precise re-scanned baselines may be necessary in situations where predictions of  $T_G$  through multi-step cure cycles are required. Except for multi-step cures, the techniques used for uncertainty estimation also appear sound and conservative.

Based on the data described thus far, there is no doubt that in cyanate esters,  $T_G$  values may significantly exceed cure temperatures, and that in these situations cure does not stop, though it clearly does slow down very significantly. To better understand these dynamics, the rates of both conversion and  $T_G$  increase were derived from the isothermal DSC data. Figures 4 and 5 present this data for catalyzed BADCy cured at 150 °C and 200 °C (after 60 minutes at 150 °C), respectively. The figures show both a linear scale over a wide range and a logarithmic scale over a narrow range of conversions corresponding to  $T_G$  values near the cure temperature. As explained previously, the error bars in these figures are based on sensitivity analyses performed on the actual data sets.

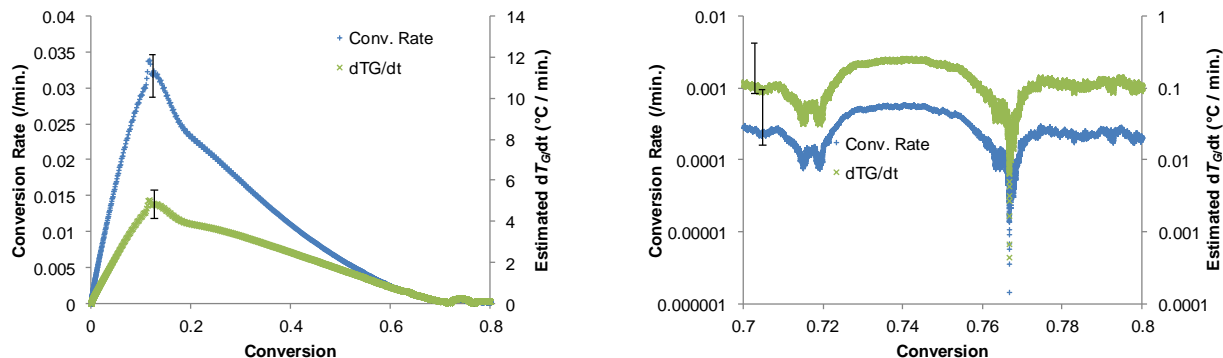


Figure 4. Conversion and  $T_G$  increase rates as a function of conversion for catalyzed BADCy cured isothermally at 150 °C. a) (left) linear scale, b) (right) logarithmic scale near the conversion ( $0.77 \pm 0.02$ ) with a corresponding  $T_G$  that matches the cure temperature. Note that the probable error ranges shown in b) are asymmetric.

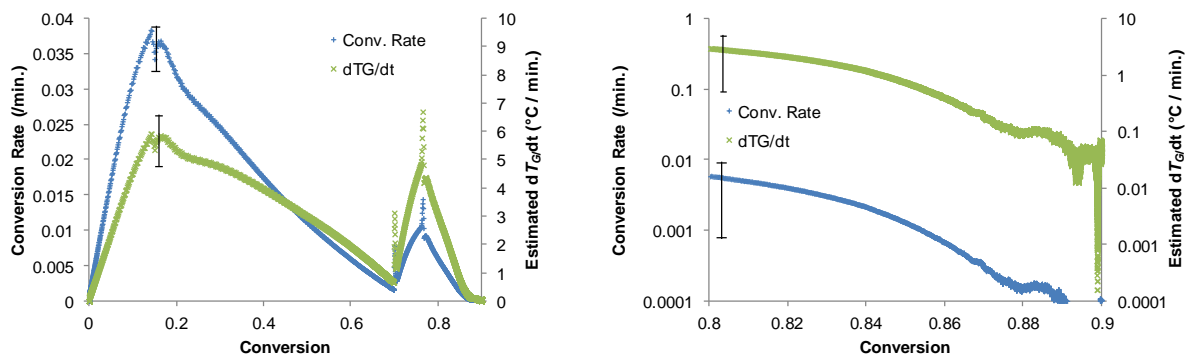


Figure 5. Conversion and  $T_G$  increase rates as a function of conversion for catalyzed BADCy cured isothermally at 150 °C for 60 minutes, followed by isothermal cure at 200 °C. a) (left) linear scale, b) (right) logarithmic scale near the conversion ( $0.86 \pm 0.01$ ) with a corresponding  $T_G$  that matches the final cure temperature. Note that the probable error ranges shown in b) are asymmetric.

A quick comparison of Figures 4 and 5 shows, as expected, that the conversion rate and  $T_G$  behavior are indeed reproducible within the error limits specified. The two peaks in Figure 5a correspond to the two isothermal segments of cure. In all cases, the rate of change of  $T_G$  follows an approximately linear dependence on conversion, with a steeper dependence at 200 °C. The conversion rate depends on conversion according to an approximate power law with an exponent that is clearly larger than one. Hamerton [11], for instance, has estimated this exponent at 2 for other data sets. Near the end of the conversion, the signal to noise ratio at 150 °C (Figure 4b) is too low to draw any conclusions about the system behavior. However, at 200 °C, where conversion rates are an order of magnitude faster, both rates appear exponentially related to conversion, with an increase in the conversion scaling factor at a point that corresponds reasonably well with the transition to sub- $T_G$ , or vitreous, curing. Such an exponential dependence of factors controlling the rate of cure, such as the diffusion coefficient, on conversion, has been previously observed for cyanate esters [12].

To see if such behavior was observed in other cyanate esters, we examined isothermal cure data for uncatalyzed ESR-255, in an experiment illustrated in Figure 6. In this case, which was originally performed as part of a chemical kinetics study [10], a re-scanned baseline is utilized for all segments of the DSC run. The isothermal portion is limited to four hours, however, the uncertainty in the  $T_G$  estimate increases rapidly during cure. Uncertainties related to diBenedetto equation parameters provide an error of 15-20 °C, and uncertainties related to baseline become

equally large at about two hours, and grow linearly to reach about 40 °C by the end of cure. This occurs because of a fundamental difference in the manner in which conversions are obtained for ESR-255. Unlike BADCy, full cure of ESR-255 in the DSC is not possible, and hence a residual cure scan does not provide the total enthalpy of conversion. Instead, as explained in our earlier study [10], a combined DSC/IR technique must be utilized to estimate the total heat of conversion. The cumulative heat flow (calibrated for accuracy using the known heat of melting of ESR-255) is then divided by this constant value to obtain the conversion estimate. Hence, the error associated with the baseline grows linearly with elapsed time, but is not divided by a corresponding integrated total that is also sensitive to baseline variation. The virtuous cancellation of error that occurs for systems with conversions estimated via residual cure thus does not take place. Moreover, because the  $T_G$  is not observable during residual cure (see Section 3.2 for an explanation), the implicit relationship between integrated heat flows and  $T_G$  established when determining the diBenedetto parameters is relied upon to provide an experimental check on the model data.

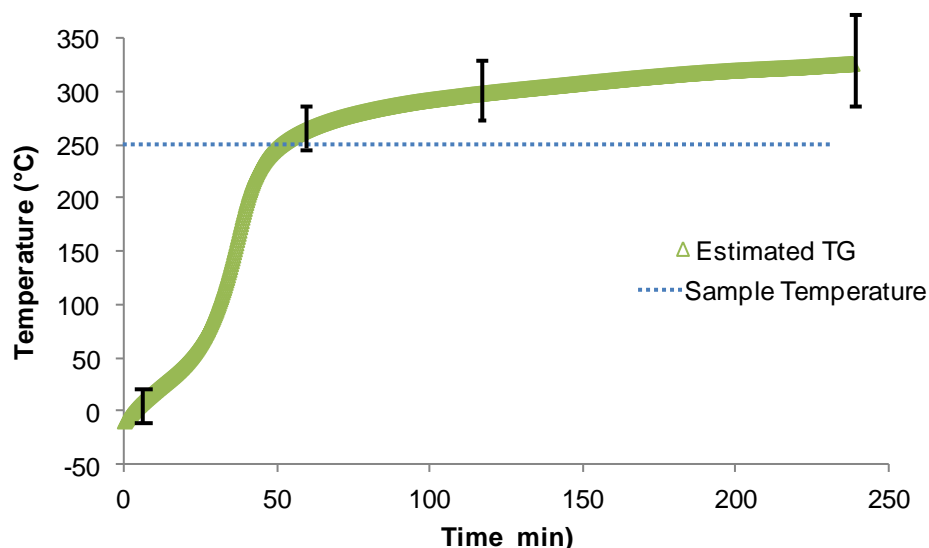


Figure 6. Estimated  $T_G$  of uncatalyzed ESR-255 during an isothermal DSC cure experiment at 250 °C.

As with BADCy, Figure 6 makes clear that the  $T_G$  exceeds the cure temperature by a significant margin and continues to rise, although the absolute rate of increase is rather uncertain. The cure kinetics of the uncatalyzed system, being auto-catalytic in nature, produce the sigmoidal feature in the  $T_G$  curve. Figure 7 shows the derived conversion and  $T_G$  increase rates as a function of conversion. Although for the overall cure, the different cure kinetics of the uncatalyzed system are evident, the cure near the glass transition temperature (Figure 7b) follows a pattern quite similar to that of BADCy. These kinetic features may thus provide the basis for a general model of cyanate ester cure that incorporates empirical formulas for sub-  $T_G$  cure.

The preceding experiments illustrate clearly that cyanate esters do cure in the glassy state. Although it seems likely that most thermosetting polymers can cure slowly in the glassy state, the high values of  $S^*$  mean that the small amount of cure that does take place in cyanate esters results in a much larger increase in  $T_G$  beyond the cure temperature. The effects of cure significantly below  $T_G$  on properties such as moisture uptake have been explored in detail by authors such as Georjon and Galy [13,14] and ourselves [15].

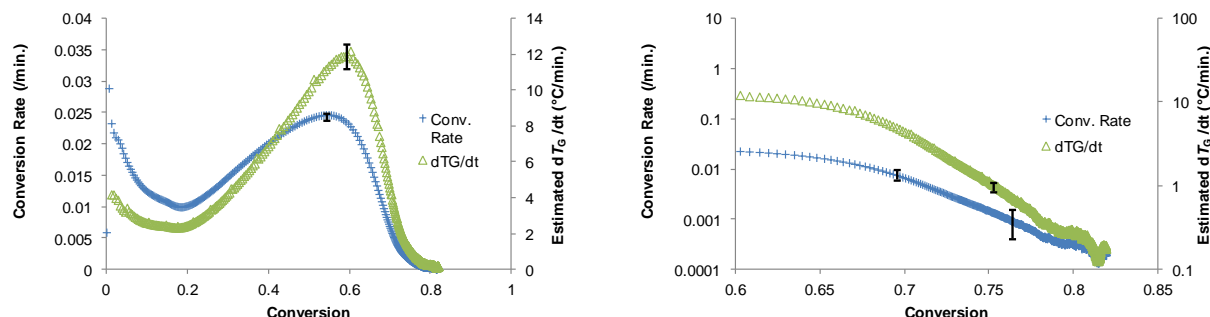


Figure 7. Conversion and  $T_g$  increase rates as a function of conversion for uncatalyzed ESR-255 cured isothermally at 250 °C. a) (left) linear scale, b) (right) logarithmic scale near the conversion ( $0.72 \pm 0.03$ ) with a corresponding  $T_g$  that matches the cure temperature.

### 3.2 Non-isothermal Cure Experiments

In addition to effects on physical properties, the fact that cyanate esters can cure well below  $T_g$  has significant implications for the measurement of  $T_g$  by techniques such as DSC, due to the phenomenon of *in-situ* cure. In order to illustrate why this is the case, Figures 8a-8c illustrate the behavior of the estimated  $T_g$  during the residual cure segment of the DSC experiments on catalyzed BADCy cured isothermally at 150 °C and 200 °C (Figures 8a and 8b), and uncatalyzed ESR-255 cured isothermally at 250 °C (Figure 8c). In these Figures, the raw DSC heat flow signals have been provided (these clearly show the “observed  $T_g$ ” values reported earlier, as well as  $T_{g\infty}$  for BADCy), along with the computed heat flow differences used to estimate changes in conversion, along with the estimated  $T_g$  values. In these figures, a dashed line indicating the coincidence of sample temperature and  $T_g$  is provided. Essentially, whenever the  $T_g$  curve crosses the dashed line, a step change in the heat flow should be evident, as is the case.

In all the examples shown, residual cure causes the  $T_g$  to rise rapidly as full conversion is approached for ESR-255 and reached for BADCy. Whereas the attainment of full conversion for BADCy causes the  $T_g$  to level off at the highest temperatures, ESR-255, being far from full conversion, shows a continuously accelerating rise in  $T_g$ . Note that even though the absolute value of  $T_g$  is quite uncertain, the rate at which it increases can be estimated reasonably well. An interesting feature to note is that for the BADCy samples, the rate at which  $T_g$  increases appears to be about the same as the heating rate, while for the ESR-255 sample, the  $T_g$  eventually increases much faster than the heating rate. These features are examined in more detail in Figure 9, in which the conversion rate and rate of increase in  $T_g$  are plotted as a function of conversion for the same set of samples used in Figure 8.

For ESR-255, the consequences of having the  $T_g$  rise faster than the sample temperature are important to consider. The post-cure DSC scan of ESR-255 shows no apparent  $T_g$  at temperatures up to 350 °C. Yet in fact only  $T_g$  values below about 300 °C can be excluded on the basis of an absence of a  $T_g$  signal, and, when one considers that the  $T_g$  could well be “buried” within the heating peak, even lower  $T_g$  values cannot be excluded with high confidence. In this case, a  $T_g$  value that might well have been detectable in the DSC is not observed because the  $T_g$  itself is a “moving target” during the scan, and in the case of ESR-255, it is a “moving target” that can easily “outrun” the sample itself, preventing its observation. This situation is in sharp contrast to that of thermoplastics, wherein the  $T_g$  is a relatively fixed value that cannot be affected much by the thermal scanning procedure.

In thermosetting polymers, the possibility of significant *in situ* cure must be considered when examining thermal analysis data. The possibility can easily be quantified using a dimensionless group, given by  $S^*(d\alpha/dt)/(dT/dt)$ , where  $dT/dt$  is the programmed heating rate of the instrument. If  $S^*$  is known for a given group material, then  $(d\alpha/dt)$  can be determined directly from the DSC output and the dimensionless group computed. For instance, in all three cases,  $d\alpha/dt$  exhibits maximum

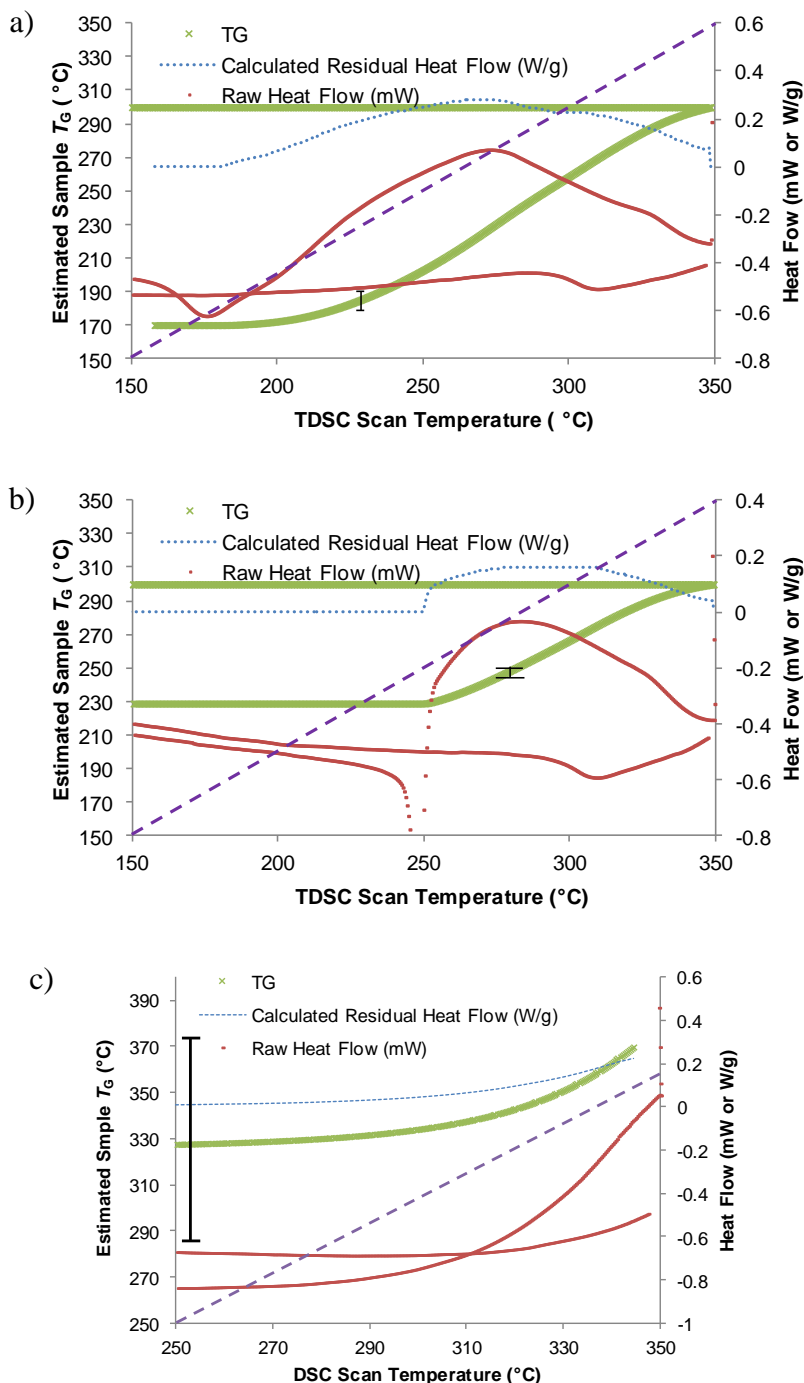


Figure 8. Raw heat flow, derived residual cure heat flow, and estimated  $T_g$  for a) catalyzed BADCy cured at 150 °C b) catalyzed BADCy cured at 200 °C, and c) uncatalyzed ESR-255 cured at 250 °C.

values between about 0.01 and 0.02 / min. For BADCy,  $S^*$  is roughly 900 °C, so that, at a heating rate of 10 °C / min., the dimensionless group ranges from 0.9 – 1.8. Since the dimensionless group may be thought of as the ratio of the rate of  $T_g$  rise to the sample heating rate, the values suggest that the rise in  $T_g$  will be roughly equal to the heating rate, which is in fact observed. Fortunately, in the “race” between  $T_g$  and the sample temperature, there is

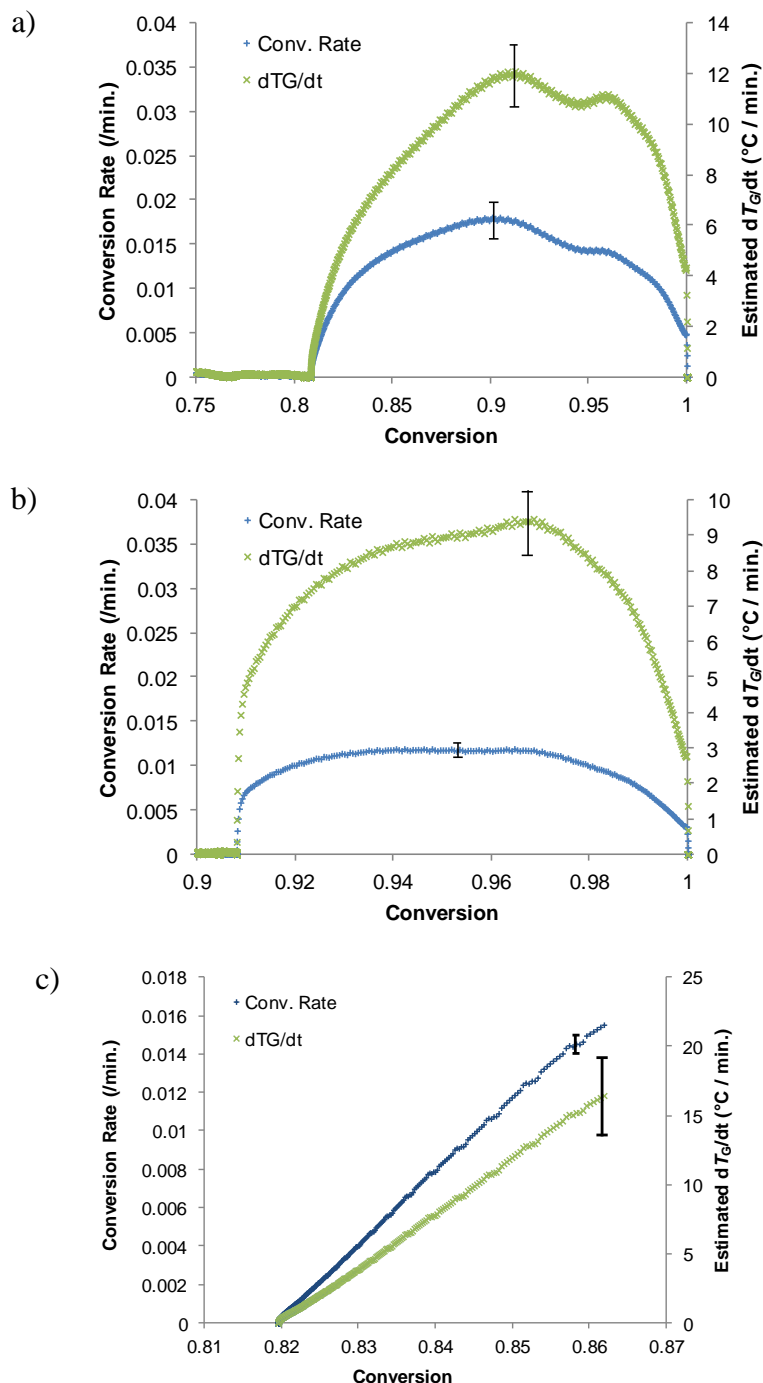


Figure 9. Conversion rate and rate of  $T_G$  increase as a function of conversion for a) catalyzed BADCy cured at 150 °C b) catalyzed BADCy cured at 200 °C, and c) uncatalyzed ESR-255 cured at 250 °C.

enough of a lag in the cure that the  $T_G$ , once encountered, never catches back up to the sample. (We have seen cases with ESR-255 and slow heating rates where the  $T_G$  does indeed catch back up, leading to a re-vitrification that can be seen in modulated DSC experiments under a narrow range of conditions). For ESR-255,  $S^*$  is much higher, at roughly 1800 °C, leading to a value range of 1.8 – 3.6 for the dimensionless group. This value, being much greater than unity, allows

ESR-255 to readily “outrun” even fast heating rates, making it a difficult material to analyze properly. (In our recent work [10], heating rates of 50 °C / min. were needed).

The need to take into account *in situ* cure and its effects means that it is important to use a variety of techniques, including DSC, when trying to understand the “as cured” state of samples. If any residual heat flow is visible in the DSC scan, then the sample  $T_G$  is a “moving target” and the “as cured” value may be significantly lower than a simple examination of the instrument readout may indicate. In other previous work [16], we showed clearly that this can be the case for catalyzed Priamset® LECy, where apparent  $T_G$  values up to 50 °C higher than the true values could be observed by using a slow heating rate. Unfortunately, slow heating rates are often viewed as more desirable for polymer samples because thermal lag is minimized. On the other hand, for many types of thermosetting resins, for which  $S^*$  is expected to be in the range of roughly 300 – 600 °C, “standard” heating rates of 3 – 5 °C are only occasionally likely to be problematic. For cyanate esters, with their unusually large  $S^*$  values, along with other emerging classes of highly processable high-temperature resins, however, this issue requires much more attention than it currently receives if the properties of these resins are to be properly measured.

## 4. CONCLUSIONS

Techniques that allow for the continuous estimation of the glass transition temperature of thermosetting polymer samples during both isothermal and non-isothermal cure have been developed and investigated. A careful analysis of uncertainties and the sensitivity of the estimates towards these sources of error showed that, with proper precautions, the  $T_G$  in many cases can be predicted to within 10 °C, and, under a broad range of conditions, to within 20 °C. The potentially most significant source of error was determining the sample baseline when several hours are required for cure. With these measurements of  $T_G$ , it has been shown that cyanate ester resins can achieve  $T_G$  values many tens of degrees higher than their cure temperature. Although the rate of conversion slows rapidly as the  $T_G$  is approached, both the conversion rate and rate of  $T_G$  increase appear to decay only exponentially as the  $T_G$  exceeds the cure temperature. As a result, finite, but slow (on the order of 0.1% / min. and 0.1 °C / min.) increases in conversion and  $T_G$  continue. When non-isothermal cure is utilized, we observed that rapid increases in  $T_G$  (often near or exceeding 10 °C/min.) took place at heating rates of 10 °C / min. As a result, the sample  $T_G$  during a non-isothermal heating (such as during a typical DSC scan) represents a “moving target” that may be encountered, if at all, at a significantly different temperature than intended. In this regard, a dimensionless group that represents the ratio of the rate of TG increases to the sample heating rate provides a useful quantitative indicator of possible issues related to *in situ* cure of samples during analysis.

## 5. REFERENCES

1. Fang, Treliaant and Shimp, David A. “Polycyanate esters: science and applications.” *Progress in Polymer Science* 20 (1995): 61-118.
2. Hamerton, Ian (Ed.). *Chemistry and Technology of Cyanate Ester Resins*. London, UK: Chapman & Hall, 1994.
3. Nair, C. P. Reghunadhan; Mathew, Dona, and Ninan, K. N. “Cyanate Ester Resins, Recent Developments.” *Advances in Polymer Science* 155 (2001): 1-99.
4. Fyfe, C. A., Niu, J., Rettig, S. J., Burlinson, N. E., Reidsema, C. E., Wang, D. W., and Poliks, M. “High Resolution  $^{13}\text{C}$  and  $^{15}\text{N}$  NMR Investigation of the Mechanism of the Curing Reactions of Cyanate-Based Polymer Resins in Solution and the Solid State.” *Macromolecules* 25 (1992): 6289-6301.

5. Reams, Josiah. T., Guenther, Andrew J., Lamison, Kevin R., Vij, Vandana, Lubin, Lisa M., and Mabry, Joseph M. "Effect of Chemical Structure and Network Formation on Physical Properties of Di(Cyanate Ester) Thermosets." *ACS Applied Materials & Interfaces* 4 (2012): 527-535.
6. Pascault, J. P. and Williams, R. J. J. "Glass transition temperature versus conversion relationships for thermosetting polymers" *Journal of Polymer Science Part B: Polymer Physics* 28 (1990): 85-95.
7. Simon, S. L., Gillham, J. K. "Cure kinetics of a thermosetting liquid dicyanate ester monomer/high  $T_g$  polycyanurate material." *Journal of Applied Polymer Science* 47 (1993): 461-485.
8. Sheng, X., Akinc, M. and Kessler, M. R. "Cure Kinetics of Thermosetting Bisphenol E Cyanate Ester." *Journal of Thermal Analysis and Calorimetry* 93 (2008): 77-85.
9. Shimp, David. A., Ising, Steven J., and Christenson, Jack R. "Cyanate Esters -- A New Family of High Temperature Thermosetting Resins" in *High Temperature Polymers and Their Uses*. Cleveland, OH: Society of Plastics Engineers, 1989, pp 127-140.
10. Guenther, Andrew J., Davis, Matthew C., Ford, Michael D., Reams, Josiah T., Groshens, Thomas J., Baldwin, Lawrence C., Lubin, Lisa M., and Mabry, Joseph M. "Polycyanurate Networks with Enhanced Segmental Flexibility and Outstanding Thermochemical Stability." *Macromolecules*, 45 (2012): 9707-9718.
11. Hamerton, I., Emsley, A. M., Howlin, B. J., Klewpatinond, P. and Takeda, S. "Studies on a dicyanate containing four phenylene rings and polycyanurate blends. 2. Application of mathematical models to the catalysed polymerization process." *Polymer* 44 (2003): 4839-4852.
12. Deng, Yong, and Martin, George C. "Diffusion phenomena during cyanate resin cure." *Polymer* 37 (1996): 3593-3601.
13. Georjon, O. and Galy, J. "Effects of crosslink density on the volumetric properties of high  $T_g$  polycyanurate networks. Consequences on moisture absorption." *Polymer* 39 (1998): 339-345.
14. Georjon, O. and Galy, J. "Effects of crosslink density on mechanical properties of high glass transition temperature polycyanurate networks." *Journal of Applied Polymer Science* 65 (1997): 2471-2479.
15. Guenther, Andrew J., Lamison, Kevin R., Vij, Vandana, Reams, Josiah T., Yandek, Gregory R., and Mabry, J. M. "New Insights into Structure-Property Relationships in Thermosetting Polymers from Studies of Co-Cured Polycyanurate Networks.", *Macromolecules* 45 (2012): 211-220.
16. Guenther, Andrew J., Lamison, Kevin R., Yandek, Gregory R., Masurat, Kenneth C., Reams, Josiah T., Cambrea, Lee R., and Mabry, Joseph M. "The role of concurrent chemical and physical processes in determining the maximum use temperature of thermosetting polymers for aerospace applications." *Polymer Preprints* 52(2) (2011): unpagged.